

ONLINE SUPPLEMENTAL MATERIAL TO:

The Gut Microbiome-Derived Metabolite Trimethylamine N-Oxide Induces Aortic Stiffening and Increases Systolic Blood Pressure with Aging in Mice and Humans

Vienna E. Brunt, Ph.D.¹, Abigail G. Casso, M.S.¹, Rachel A. Gioscia-Ryan, Ph.D., M.D.¹, Zachary J. Sapinsley, M.S.¹, Brian P. Ziemba, Ph.D.¹, Zachary S. Clayton, Ph.D.¹, Amy E. Bazzoni, B.A.¹, Nicholas S. VanDongen, M.S.¹, James J. Richey, M.S., M.P.H.¹, David A. Hutton, B.A.¹, Melanie C. Zigler, M.S.¹, Andrew P. Neilson, Ph.D.^{2*}, Kevin P. Davy, Ph.D.³, and Douglas R. Seals, Ph.D.¹

¹ Department of Integrative Physiology, University of Colorado Boulder, Boulder, CO

² Department of Food Science and Technology, Virginia Tech, Blacksburg, VA

³ Department of Human Nutrition, Foods, and Exercise, Virginia Tech, Blacksburg, VA

*Andrew Neilson's current affiliation is Department of Department of Food, Bioprocessing and Nutrition Sciences, North Carolina State University, Kannapolis, NC

SUPPLEMENTAL METHODS

Human aortic stiffness

Aortic stiffness was assessed by carotid-femoral pulse wave velocity (c-f PWV) per American Heart Association guidelines¹ via applanation tonometry with simultaneous ECG gating of the R-wave (Non-Invasive Hemodynamics Workstation, Cardiovascular Engineering Inc., Norwood, MA). Using the R-wave as the reference point, the arterial pressure wave transit time was determined as the time delay (in seconds) to the onset of the arterial pressure wave obtained by tonometry between the common carotid and femoral arteries. Distance traveled by the arterial pressure wave was estimated by subtracting the distance from the sternal notch (SN) to the common carotid artery (CCA) recording site from that of the SN to the femoral artery (FA) recording site (i.e., distance = [SN to FA] – [SN to CCA]). c-f PWV was calculated as the distance traveled (m) divided by the time delay between the arterial pressure wave transit times at each site.

Mouse *in vivo* aortic stiffness

Mice were anesthetized under 2% isoflurane and placed supine with paws secured to ECG electrodes on a heated board (37°C). Doppler ultrasound probes were used to non-invasively detect arterial waveforms at the transverse aortic arch and abdominal aorta. Aortic (a)PWV was calculated as the direct distance between arterial recording sites (cm) divided by the difference in the time delay (in seconds) from the ECG R-wave to the onset of each velocity waveform (Doppler Signal Processing Workstation, Indus Instruments, Webster, TX).

Mouse aortic stress-strain testing

As *in vivo* arterial stiffness is influenced by various factors, including autonomic tone, blood pressure and humoral factors, intrinsic mechanical stiffness and elasticity of the mouse aorta were assessed in isolated 1-2 mm segments of thoracic aorta that were collected at time of sacrifice, cleaned of surrounding tissue, and stored at -80°C in phosphate buffered saline (PBS) until later use. The segments were loaded onto a wire myograph (DMT, Inc.; Aarhus, Denmark) in heated (37°C) PBS and were pre-stretched to a 1 mm luminal diameter and returned to the initial non-stretched position 3 times. Subsequently, the force (mN) was measured as the vessel was stretched 50 µm incrementally (every 3 minutes) until reaching the point of mechanical failure, which was determined as the point at which force suddenly decreased. A stress-strain curve was generated in which strain and stress were defined as the following:

$$\text{Strain } (\lambda) = \Delta d/d(i)$$

* d = diameter; $d(i)$ = initial diameter

$$\text{Stress } (t) = \lambda L/2HD$$

* L = one-dimensional load; H = intima-media thickness; D = vessel length

The diameter (d) and intima-media thickness (H) of the samples were determined using ~1 mm sections of mouse thoracic aorta collected at time of sacrifice. These samples were frozen in optimal cutting temperature (OCT) compound in liquid nitrogen-cooled methylbutane and stored at -80°C. The samples were later sectioned (7 µM; Leica CM3000, Leica Biosystems Inc., Lincolnshire, IL), plated on microscope slides, imaged using a Nikon Eclipse TS100, and analyzed using ImageJ software (National Institutes of Health, Bethesda, MA). The medial and adventitial layers were distinguished by

determining where the regular banding patterns (media) abruptly shifted to diffuse patterning (adventitia).

Elastic moduli of the stress-strain curve were determined as summarized in **Supplemental Figure S1**. To determine aortic intrinsic stiffness, the final four points of the stress-strain curve were fitted to a linear equation ($r^2 > 0.99$), which defined the high-force collagen-dominant region of the elastic modulus (EM)²⁻⁶. To determine aortic intrinsic elasticity, the low-force elastin-dominant region of the EM was determined by fitting a seventh order polynomial equation to the data to calculate the roots (RStudio; Foundation for Statistical Computing, Vienna, Austria). The elastin region of the EM was defined as the slope of a linear equation ($r^2 > 0.99$) fit to the stress-strain curve between the first and second roots: the first root considered the intersect between the very low force region and the elastin region, and the second root considered the intersect between the elastin region and the initial activation of collagen fibers³⁻⁵.

Western Immunoblotting in mouse aorta lysates

Protein abundance was determined in mouse thoracic aorta lysates using either traditional Western immunoblotting or capillary electrophoresis Western detection using a WES instrument (ProteinSimple, San Jose, CA). Traditional Western immunoblotting was used for assessment of advanced glycation end products (AGEs), as we have not yet found an antibody that reliably detects AGEs on WES. Protein (20 μ g) was loaded onto SDS gels and separated via electrophoresis. The samples were transferred onto nitrocellulose membranes, incubated for ≥ 1 hour in blocking buffer containing tris-buffered saline with tween (TBS-T) with 5% w/v dry milk powder, and then incubated overnight at 4°C with primary antibodies. The following day, the samples were washed 3 times with TBS-T and incubated with a horseradish peroxidase-conjugated secondary antibody at room temperature for 1 hour. The samples were washed 3 times with TBS-T, incubated in ECL Western Blotting Substrate (ThermoFisher Scientific, Inc., Waltham, MA), and target proteins detected by chemiluminescent imaging. Primary antibodies were anti-AGEs (1:1000; Abcam, Cambridge, UK; Cat# AB23722) and anti-glyceraldehyde 3-phosphate dehydrogenase (GAPDH; 1:1000; Cell Signaling Technology, Inc., Danvers, MA; Cat# 14C10). AGEs abundance was measured as relative intensity normalized to the GAPDH intensity.

Capillary electrophoresis Western detection (WES instrument) was used for assessment of collagen and elastin. Proteins (0.25 μ g/ μ l) were separated by capillary electrophoresis, and immunodetection was performed, both of which were done automatically using the default settings, except for the primary antibody incubation phase, which was extended to 150 min. Aliquoting of the samples, blocking reagent, wash buffer, primary antibodies, secondary antibodies, and chemiluminescent substrate were completed by the instrument. The data was analyzed using the installed Compass software (ProteinSimple). Primary antibodies were anti-collagen type I (1:10; Abcam; Cat# AB21286), anti-elastin (1:20; ThermoFisher Scientific, Inc., Waltham, MA; Cat# PA5 72440), and anti-GAPDH (1:200, Cell Signaling Technology; Cat# 14C10). Protein abundance was determined as intensity of the band normalized against intensity of GAPDH signal. Electropherograms shown in figures are pseudo blots generated by the Compass software.

Immunohistochemistry in mouse aortas

The protein abundance and localization of collagen and AGEs were assessed using ~1 mm sections of mouse thoracic aorta which were collected at time of sacrifice, frozen in OCT compound and stored as described above. At a later time, the samples were sectioned (7 μ M; Leica CM3000, Leica Biosystems Inc.) and plated on poly-L-lysine coated slides, fixed in 3.7% paraformaldehyde and

stored at -80°C until further use in immunohistochemical analyses. Upon staining, the slides were rehydrated (PBS + 50 mM glycine), washed with PBS, permeabilized (0.1% Triton X-100), and incubated for 20 minutes with 2.5% normal horse serum blocking buffer following 3 washes with PBS. Slides were then incubated with primary antibodies at room temperature for 1 hour, washed 3 times with PBS, incubated with a horseradish peroxidase-conjugated secondary antibody for 30 minutes, treated with 1:1 3,3'-Diaminobenzidine (DAB): H_2O_2 for approximately 8 minutes as the samples began to darken, and then immediately washed in PBS and cured overnight with gelvatol. The slides were imaged using a Nikon Eclipse TS100 under identical conditions and analyzed using ImageJ software. The medial and adventitial layers were distinguished as described above. Protein abundance was measured as relative intensity normalized to the background intensity. Primary antibodies for aortic protein targets were anti-collagen I (1:1000; Novus Biologicals LLC, Centennial, CO; Cat# NB600-450) and anti-AGEs (1:200; Abcam; Cat# AB23722).

Statistical Analyses

Young vs. middle-aged to older (MA/O) comparisons in humans. Differences in the following variables between young and MA/O adults were compared using Student's unpaired t-test: plasma concentrations of TMAO and related metabolites, c-f PWV, systolic and diastolic blood pressures, and the subject characteristics reported in Supplemental Table S1.

Human arterial stiffness or blood pressure and plasma TMAO linear regression analysis. Regression analyses were performed similarly between c-f PWV, systolic blood pressure (SBP), or diastolic blood pressure (DBP) and plasma TMAO using data from MA/O (c-f PWV, N=83; SBP/DBP, N=101) and young subjects (c-f PWV, N=14; SBP/DBP, N=21). TMAO and c-f PWV values were natural log-transformed due to skewness in the data (Shapiro-Wilk test, TMAO: $p < 0.0001$; c-f PWV: $p = 0.003$). First, simple linear (unadjusted) regressions were performed between c-f PWV, SBP, DBP and Ln plasma TMAO. Next, in c-f PWV or SBP (DBP not included as no relation existed in the previous model) were regressed onto Ln plasma TMAO with 1) the following traditional cardiovascular risk factors as covariates: sex, body mass index, cardiorespiratory fitness (VO_2max), serum total cholesterol and LDL cholesterol, and fasted blood glucose; 2) [for c-f PWV only] these cardiovascular risk factors and mean arterial pressure; 3) age as a covariate in addition to all cardiovascular risk factors listed; and 4) all cardiovascular risk factors, age, and the number of anti-hypertensive medications subjects were taking (i.e., 0, 1, or 2). P-values for the main effect of TMAO in each model were calculated. To determine the independent effect of TMAO after accounting for all covariates, we determined multivariable partial relations (partial r^2 of TMAO) by calculating the correlation between the residuals of TMAO and the residuals of c-f PWV or SBP in each multiple regression. Select regressions were rerun with subsets of just the young or MA/O subjects included, as summarized in Supplemental Table S3 below.

Power calculations for animal studies. Power calculations were performed using G-power based on aPWV data collected previously in our laboratory. Group sizes of N=10 mice per condition are sufficient to detect differences in aPWV with 95% power using $\alpha = 0.01$. To ensure we would obtain successful aPWV tracings pre and post intervention from 10 mice/group, starting group sizes were N=12/group. Starting group sizes of old mice were increased by 50% to account for attrition over the course of the intervention. Of the 36 old mice obtained from the National Institute on Aging for this study, 11 died prior to the start of the intervention and 6 died during the intervention (2 control, 4 TMAO-supplemented), and 19 were studied post-intervention. i.e., 22% attrition. Deaths were expected due to old age but appeared to be exacerbated by TMAO supplementation.

Comparisons across age and treatment groups in mice. Differences in the following variables across the 4 age and treatment groups (young Control, young TMAO, old Control, and old TMAO) were compared using one-way analysis of variance (ANOVA): body mass, food intake, mass of key organs, plasma concentrations of TMAO and related metabolites. Differences in aPWV and blood pressures were determined separately within each age group using two-way mixed design ANOVA with a between factor of group (Control vs. TMAO) and repeated factor of time into the intervention. For both sets of analyses, when significant main effects were detected, pairwise comparisons were made using Tukey's post-hoc test. Differences in aortic intrinsic mechanical stiffness and elasticity and abundance of all protein targets (Western immunoblotting and immunohistochemistry) were determined across young Control vs. TMAO-supplemented mice using Student's unpaired t-test.

Direct TMAO incubations in mouse aortic rings. Differences in intrinsic aortic stiffness following incubation with TMAO vs. vehicle were compared using Student's paired t-test. Effects of pharmacological compounds on TMAO-induced intrinsic stiffening were determined using two-way repeated measures ANOVA with factors of treatment (Vehicle vs. TMAO) and pharmacological agent (Vehicle alone vs. alagebrium or TEMPOL). When significant main effects were detected, pairwise comparisons were made using Sidak's multiple comparisons test.

SUPPLEMENTAL REFERENCES

1. Townsend RR, Wilkinson IB, Schiffrin EL, Avolio AP, Chirinos JA, Cockcroft JR, Heffernan KS, Lakatta EG, McEniery CM, Mitchell GF, Najjar SS, Nichols WW, Urbina EM, Weber T, American Heart Association Council on Hypertension. Recommendations for improving and standardizing vascular research on arterial stiffness: A scientific statement from the American Heart Association. *Hypertension* 2015; **66**:698-722.
2. Fleenor BS, Sindler AL, Eng JS, Nair DP, Dodson RB, Seals DR. Sodium nitrite de-stiffening of large elastic arteries with aging: role of normalization of advanced glycation end-products. *Exp Gerontol* 2012; **47**:588–594.
3. Gioscia-Ryan RA, Battson ML, Cuevas LM, Eng JS, Murphy MP, Seals DR. Mitochondria-targeted antioxidant therapy with MitoQ ameliorates aortic stiffening in old mice. *J Appl Physiol* 2018; **124**:1194–1202.
4. Brunt VE, Gioscia-Ryan RA, Richey JJ, Zigler MC, Cuevas LM, González A, Vázquez-Baeza Y, Battson ML, Smithson AT, Gilley AD, Ackermann G, Neilson AP, Weir T, Davy KP, Knight R, Seals DR. Suppression of the gut microbiome ameliorates age-related arterial dysfunction and oxidative stress in mice. *J Physiol* 2019; **597**:2361–2378.
5. Lammers SR, Kao PH, Qi HJ, Hunter K, Lanning C, Albiets J, Hofmeister S, Mecham R, Stenmark KR, Shandas R. Changes in the structure-function relationship of elastin and its impact on the proximal pulmonary arterial mechanics of hypertensive calves. *Am J Physiol Heart Circ Physiol* 2008; **295**:H1451–H1459.
6. Sokolis DP, Boudoulas H, Karayannacos PE. Assessment of the aortic stress-strain relation in uniaxial tension. *J Biomech* 2002; **35**:1213–1223.

SUPPLEMENTAL TABLES

Supplemental Table S1. Coefficients of variation for mass spectrometry analytes

Analyte	Average	Range
TMAO standard	4.2 %	1.4 – 6.2 %
Deuterated 9d-TMAO	4.6 %	3.6 – 6.2 %
Choline standard	3.5 %	0.5 – 8.1 %
Deuterated 9d-Choline	4.0 %	2.0 – 7.6 %
Betaine standard	5.3%	1.5 – 8.5 %
Deuterated 11d-Betaine (1)	6.6 %	1.5 – 9.6 %
Deuterated 11d-Betaine (2)	6.1 %	3.3 – 7.9 %
L-Carnitine standard	6.4 %	5.1 – 8.1 %
Deuterated 9d-L-Carnitine	4.9 %	2.7 – 7.6 %

Percent coefficients of variation for individual non-isotopic (“standard”) and radioisotope (“deuterated”) analyte measurements spiked into calibration plasma (for isotope measurements) and test plasma (for standard measurements). Average %CV values represent averages of variation in isotopic compound signal when assessing isotopic metabolite standards spiked into each quality control standard and unknown plasma sample, while variation of non-isotopic compounds were assessed in repeated measurements of quality control standard plasma that was assessed before and after every 5 unknown plasma sample measurements.

Supplemental Table S2. Human subjects' characteristics, medications, and plasma concentrations of TMAO precursors

Characteristic, Medication or TMAO Precursor	Young		MA/O	
	Whole cohort (N=21)	c-f PWV subgroup (N=14)	Whole cohort (N=101)	c-f PWV subgroup (N=83)
<i>Subject characteristics</i>				
Age (yrs)	22 ± 2	22 ± 1	64 ± 7*	64 ± 7*
Men/women	11/10	10/4	44/57	38/45
Body mass (kg)	68 ± 10	72 ± 7	70 ± 14	69 ± 14
Height (cm)	172 ± 9	175 ± 7	170 ± 9	171 ± 8
Body mass index (kg/m ²)	22.9 ± 2.2	23.7 ± 2.1	23.9 ± 3.6	23.6 ± 3.4
VO ₂ max (ml/min/kg)	45.8 ± 9.3	45.4 ± 8.1	30.5 ± 5.8*	31.3 ± 5.4*
Total cholesterol (mg/dL)	153 ± 28	155 ± 33	181 ± 29*	182 ± 29*
LDL cholesterol (mg/dL)	85 ± 25	89 ± 28	107 ± 26*	108 ± 27*
HDL cholesterol (mg/dL)	52 ± 12	50 ± 11	56 ± 16	56 ± 17
Triglycerides (mg/dL)	86 ± 44	85 ± 51	91 ± 49	93 ± 48
Glucose (mg/dL)	78 ± 10	79 ± 11	86 ± 8*	86 ± 8*
Serum creatinine (mg/dL)	0.9 ± 0.1	0.9 ± 0.1	0.9 ± 0.2	0.9 ± 0.2
Estimated GFR (ml/min/1.73 m ²)	96 ± 11	97 ± 12	77 ± 15*	78 ± 15*
<i>Circulating inflammatory markers</i>				
C-reactive protein (mg/L)	0.7 ± 0.6	1.1 ± 1.1	0.6 ± 0.4	1.0 ± 0.9
Interleukin-6 (pg/mL)	0.8 ± 0.3	1.1 ± 0.5	0.8 ± 0.3	1.0 ± 0.5
<i>Medications (number and % of subjects)</i>				
None	15 (71%)	11 (79%)	56 (55%)	43 (52%)
Blood-pressure lowering	0	0	14 (14%)	14 (17%)
Cholesterol-lowering	0	0	12 (12%)	12 (14%)
Thyroid medications	1 (5%)	0	11 (11%)	9 (11%)
Aspirin/NSAIDs	0	0	10 (10%)	9 (11%)
SSRIs	0	0	8 (8%)	7 (8%)
ADHD medications	2 (10%)	1 (7%)	2 (2%)	2 (2%)
Contraceptives	4 (19%)	2 (14%)	0	0
Others	0	0	11 (11%)	10 (12%)
<i>Plasma concentrations of TMAO precursors</i>				
Choline	7.8 ± 3.1	7.7 ± 3.4	13.9 ± 6.1*	14.1 ± 6.5*
Betaine	18.6 ± 10.6	18.7 ± 10.3	20.1 ± 12.1	21.7 ± 12.9
L-carnitine	48.4 ± 14.3	49.6 ± 16.4	57.3 ± 31.1	55.5 ± 28.4

Characteristics for all human subjects (whole cohort; for plasma TMAO and blood pressure) and those with measurements of carotid-femoral pulse wave velocity (c-f PWV subset). Circulating inflammatory markers were measured in fewer subjects: n=16 young adults, of which 14 had c-f PWV measured (both markers); in MA/O adults, C-reactive protein was measured in n=93, of which 79 had c-f PWV measured, and interleukin-6 was measured in n=85, of which 73 had c-f PWV measured. Data are mean ± S.D. Young: age 18-27; middle-aged to older (MA/O): age 45-79. *p<0.05 vs. young. Within each age group, there were no differences between the whole cohort and the subset of subjects. Abbreviations: TMAO, trimethylamine N-oxide; GFR, glomerular filtration rate; NSAIDs, non-steroidal anti-inflammatory drugs; SSRIs, selective serotonin reuptake inhibitors; ADHD, attention-deficit/hyperactivity disorder. Other medications include (one subject taking each one): Maxalt, Sumatriptan, Wellbutrin, Ambien, Lorazepam, Asmanex, Effexor, Lamictal, Skelaxin, Uloric, Allopurinol, Nexium, and Detrol.

Supplemental Table S3. Full results of multiple linear regression analyses

Regression Model	Full cohort (N=97-122)		Young only (N=14-21)		MA/O only (N=83-101)	
	Partial r ²	P-value	Partial r ²	P-value	Partial r ²	P-value
PWV ~ TMAO	0.17	<0.0001**	0.44	0.01*	0.07	0.02*
PWV ~ TMAO + CV risk factors	0.09	0.004**	0.75	0.006**	0.05	0.06
PWV ~ TMAO + CV risk factors + MAP	0.07	0.01*	0.66	0.03*	0.02	0.23
PWV ~ TMAO + CV risk factors + Age	0.005	0.51	0.74	0.01*	0.02	0.23
PWV ~ TMAO + CV risk factors + Age + MAP	0.004	0.57	0.69	0.04*	0.007	0.48
SBP ~ TMAO	0.09	0.0008**	0.16	0.07	0.06	0.02*
SBP ~ TMAO + CV risk factors	0.05	0.02*	0.14	0.18	0.04	0.048*
SBP ~ TMAO + CV risk factors + Age	0.004	0.51	0.05	0.46	0.02	0.18
DBP ~ TMAO	0.02	0.11	0.15	0.09	0.01	0.26

Abbreviations: CV, cardiovascular; DBP, diastolic blood pressure; MA/O, middle-aged to older adults; MAP, mean arterial pressure; PWV, pulse wave velocity; SBP, systolic blood pressure; TMAO, trimethylamine N-oxide. Multiple linear regression analyses were performed for each model, with the dependent variable (PWV, SBP, or DBP) indicated first, followed by all independent variables. TMAO and PWV were natural log transformed prior to analyses to account for skewness. In each model, the independent effect of TMAO after accounting for all covariates was determined by multivariable partial relations (partial r²). P-values provided are for the effect of TMAO in each model. *p<0.05, **p<0.05. CV risk factors included sex, body mass index, cardiorespiratory fitness (VO₂max), total cholesterol, low-density lipoprotein cholesterol, and blood glucose.

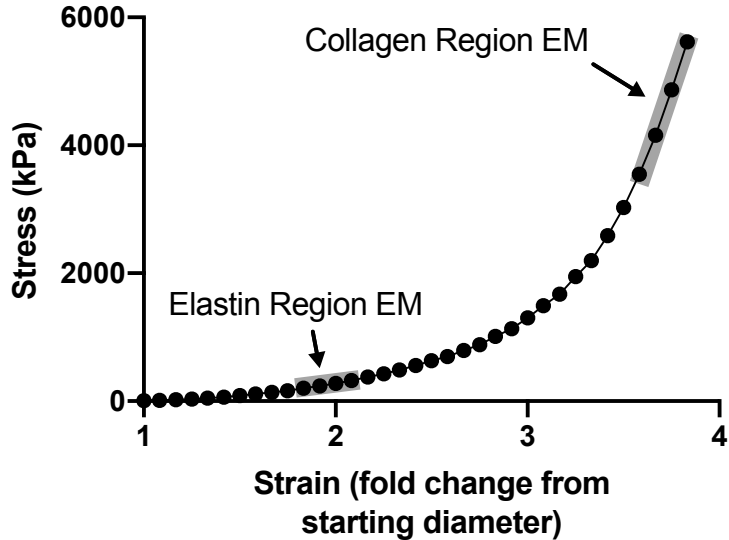
Supplemental Table S4. Chronic TMAO supplementation mouse study: Animal characteristics and concentrations of TMAO-related metabolites

Characteristic or Metabolite	YC	YT	OC	OT
Body mass (g)	40 ± 2	42 ± 2	29 ± 2*	30 ± 2*
Food intake (kcal/day)	15.0 ± 0.2	15.4 ± 0.3	14.8 ± 0.3	15.1 ± 0.3
<i>Mass of key organs</i>				
Heart mass (mg)	158 ± 8	160 ± 4	166 ± 7	159 ± 8
Liver mass (g)	1.89 ± 0.14	2.09 ± 0.14	1.39 ± 0.05*	1.49 ± 0.07
Kidney mass (mg)	206 ± 10	216 ± 7	214 ± 13	210 ± 13
Visceral fat mass (g)	2.16 ± 0.23	2.15 ± 0.19	0.55 ± 0.23*	0.58 ± 0.23*
<i>Concentrations of TMAO-related metabolites</i>				
Choline (μM)	25 ± 3	28 ± 4	153 ± 18*	161 ± 39*
Betaine (μM)	12 ± 11	14 ± 2	13 ± 1	13 ± 1
L-carnitine (μM)	24 ± 6	20 ± 3	22 ± 1	20 ± 1
γ-butyrobetaine (μM)	1.0 ± 0.2	1.0 ± 0.2	1.2 ± 0.2	0.9 ± 0.2

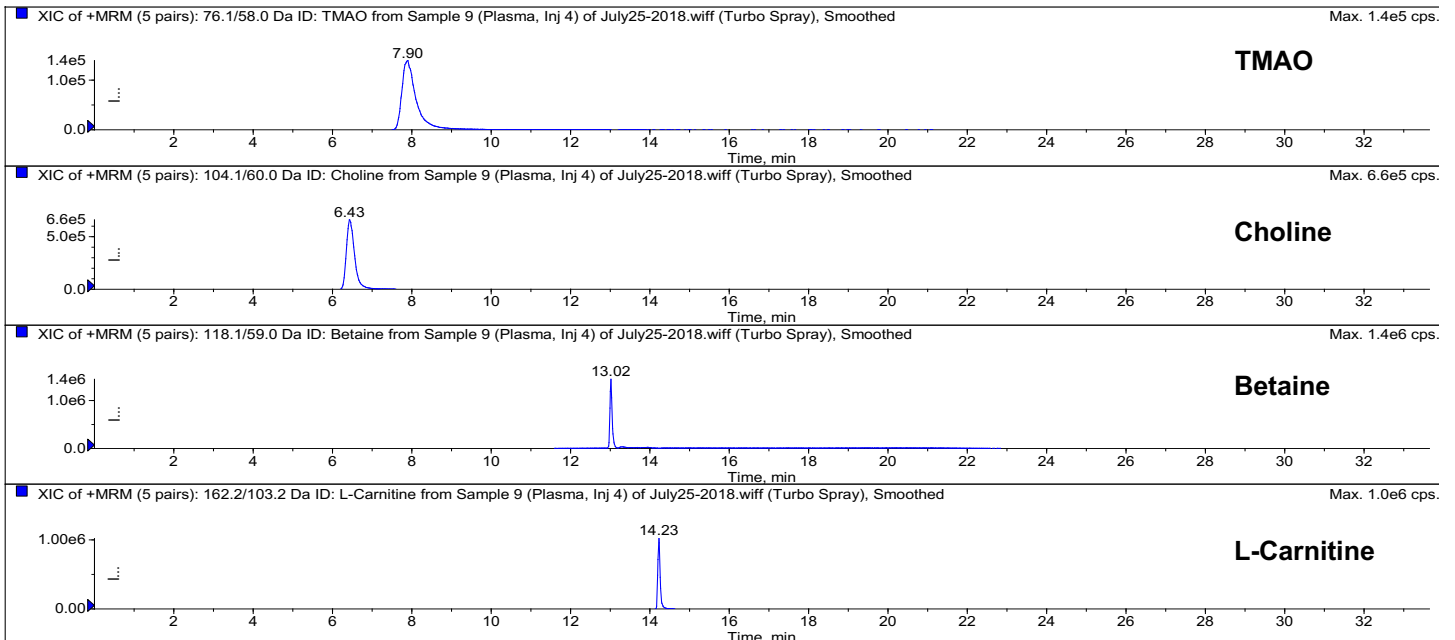
Data are mean ± S.E.M. N=9-11/group. *p<0.05 vs. YC. Abbreviations: TMAO, trimethylamine N-oxide; YC, young control; YT, young TMAO-supplemented; OC, old control; OT, old TMAO-supplemented.

SUPPLEMENTAL FIGURES

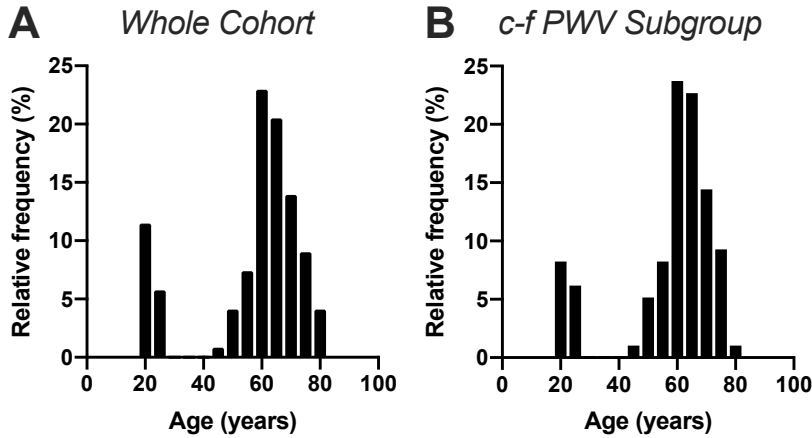
Supplemental Figure S1. Representative stress-strain curve for assessment of aortic intrinsic mechanical stiffness and elasticity. Abbreviation: EM, elastic modulus.



Supplemental Figure S2. Representative multiple reaction monitoring (MRM) traces of non-isotopic fragment ions in human plasma extract. The traces depict the specific separation of the individual compounds where all compounds are present in the sample matrix. The separation allows for specific monitoring of individually selected metabolites, as depicted.



Supplemental Figure S3. Histogram of the age distribution among subjects in the entire cohort (N=122; **A**) and in the subgroup with carotid-femoral pulse wave velocity (c-f PWV) measurements (N=97; **B**). Ages are binned into 5-year intervals. The distribution of middle-aged to older adults (ages 45-79) was normally distributed.



Supplemental Figure S4. Chronic trimethylamine N-oxide (TMAO) supplementation increases diastolic blood pressure (BP) in young and old mice. *In vivo* tail cuff diastolic BP in **A**) young adult (6-12 months of age) and **B**) old (21-24 months) mice supplemented without (Control; YC, OC) or with 0.12% TMAO (YT, OT) for 3-6 months. Data are mean \pm S.E.M. **C**) Individual data from young and old mice at the post-intervention time point (6 months for young adult mice; 3 months for old mice). Differences across groups were compared using two-way mixed design ANOVA. P-values are pairwise comparisons (Tukey's post-hoc test). * $p < 0.05$ vs. Control, within time point/age group. † $p < 0.05$ vs. baseline (0 months on intervention), within group. Abbreviations: YC, young control; YT, young TMAO-supplemented; OC, old control; OT, old TMAO-supplemented.

